ISSN 0006-2979, Biochemistry (Moscow), 2008, Vol. 73, No. 8, pp. 886-896. © Pleiades Publishing, Ltd., 2008.
Original Russian Text © Yu. S. Krasikova, N. I. Rechkunova, E. A. Maltseva, I. O. Petruseva, V. N. Silnikov, T. S. Zatsepin, T. S. Oretskaya, O. D. Scharer, O. I. Lavrik, 2008, published in Biokhimiya, 2008, Vol. 73, No. 8, pp. 1101-1113.
Originally published in Biochemistry (Moscow) On-Line Papers in Press, as Manuscript BM07-426, July 6, 2008.

Interaction of Nucleotide Excision Repair Factors XPC–HR23B, XPA, and RPA with Damaged DNA

Yu. S. Krasikova[1,2], N. I. Rechkunova[1], E. A. Maltseva[1], I. O. Petruseva[1], V. N. Silnikov[1], T. S. Zatsepin[3], T. S. Oretskaya[3], O. D. Scharer[4], and O. I. Lavrik[1,2]*

[1]*Institute of Chemical Biology and Fundamental Medicine, Siberian Branch of the Russian Academy of Sciences, pr. Lavrentieva 6, 630090 Novosibirsk, Russia; fax: (383) 333-3677; E-mail: lavrik@niboch.nsc.ru*
[2]*Novosibirsk State University, ul. Pirogova 2, 630090 Novosibirsk, Russia*
[3]*Faculty of Chemistry, Lomonosov Moscow State University, 119992 Moscow, Russia*
[4]*Department of Pharmacological Sciences, SUNY Stony Brook, Stony Brook, New York 11794-3400, USA; E-mail: Orlando@pharm.stonybrook.edu*

Received December 20, 2007
Revision received March 18, 2008

Abstract—The interaction of nucleotide excision repair factors—xeroderma pigmentosum complementation group C protein in complex with human homolog of yeast Rad23 protein (XPC–HR23B), replication protein A (RPA), and xeroderma pigmentosum complementation group A protein (XPA)—with 48-mer DNA duplexes imitating damaged DNA structures was investigated. All studied proteins demonstrated low specificity in binding to damaged DNA compared with undamaged DNA duplexes. RPA stimulates formation of XPC–HR23B complex with DNA, and when XPA and XPC–HR23B are simultaneously present in the reaction mixture a synergistic effect in binding of these proteins to DNA is observed. RPA crosslinks to DNA bearing photoreactive 5I-dUMP residue on one strand and fluorescein-substituted dUMP analog as a lesion in the opposite strand of DNA duplex and also stimulates cross-linking with XPC–HR23B. Therefore, RPA might be one of the main regulation factors at various stages of nucleotide excision repair. The data are in agreement with the cooperative binding model of nucleotide excision repair factors participating in pre-incision complex formation with DNA duplexes bearing damages.

DOI: 10.1134/S0006297908080063

Key words: nucleotide excision repair factors, photoaffinity labeling, photoreactive oligonucleotides, complex formation

Transfer of genetic information without alterations is necessary for the survival of cells as well as that of the whole organism. However, the integrity of DNA, the main carrier of genetic information, is constantly jeopardized by many external and internal agents damaging its structure. Many DNA lesions and mutations can result from the action of these agents; this may cause the progress of cancer and other diseases. Several mechanisms restoring damaged DNA were developed by living organisms in the course of evolution. The nucleotide excision repair (NER) system is one of these mechanisms. The ability to remove a wide range of DNA lesions is typical of NER, in particular, in mammal cells this is the major repair pathway to eliminate bulky DNA adducts appearing either by the action of environmental factors, such as UV irradiation and chemical carcinogens, or as a result of chemotherapeutic treatment [1-4]. Mutations in NER-related genes cause several hereditary diseases, such as xeroderma pigmentosum (XP), Cockayne syndrome, and trichothiodystrophy [4]. Patients with XP syndrome are highly sensitive to sunlight, and many of them develop skin cancer [5-7].

There are two NER pathways in eukaryotic cells: transcription-coupled repair (TC-NER), which restores DNA strands of actively transcribed genes, and global genome repair (GG-NER) restoring DNA in nontran-

Abbreviations: Flu-dUMP) 5-{3-[6-(carboxyamido-fluoresceinyl)amidocapromoyl]allyl}-2′-deoxyuridine 5′-monophosphate; 5I-dUMP) 5-iodo-2′-deoxyuridine 5′-monophosphate; NER) nucleotide excision repair; RPA) replication protein A; XP) xeroderma pigmentosum; XPA) xeroderma pigmentosum complementation group A protein; XPC–HR23B) xeroderma pigmentosum complementation group C protein in complex with human homolog of yeast Rad23 protein.

* To whom correspondence should be addressed.

scribed parts of the genome [8]. More than 30 polypeptides participate in NER at its various stages, namely: i) lesion recognition; ii) unwinding of DNA duplex around the damaged area; iii) cleavage of the damaged DNA strand at the 3′- and 5′-ends of the lesion; iv) gap filling; v) nick ligation [1, 2, 9].

NER pathways differ mainly in the lesion recognition stage. In the case of TC-NER, the lesion is recognized on its interaction with RNA polymerase II and transcription termination [10, 11]. It is still unclear how the GG-NER system recognizes lesions. According to a model suggested by Evans et al. [12], a lesion is primarily recognized by xeroderma pigmentosum complementation group C protein in complex with human homolog of yeast Rad23 protein (XPC–HR23B). This model was supported in experiments in which cell extracts depleted in NER factors were used [13]. It was shown that damaged DNA preincubated with XPC–HR23B is processed more rapidly than DNA preincubated with xeroderma pigmentosum complementation group A protein in complex with replication protein A (XPA–RPA). According to the suggested model, GG-NER is processed via a mechanism in which XPC–HR23B complex acts as a factor recognizing the lesion-induced change in DNA helix conformation and providing subsequent recruitment of repair/transcriptional factor TFIIH to the complex formed. At the next stage, XPB and XPD helicases of TFIIH unwind the DNA duplex, then XPA–RPA complex verifies chemical modifications, and the above-described stages 3-5 proceed [12, 13]. However, contrary results were obtained in an NER system reconstructed *in vitro* from the purified proteins: substrate preincubated with XPA–RPA complex was processed more rapidly [14]. Based on these data, an alternative model of NER was suggested; according to this model, primary recognition of a lesion is performed by XPA–RPA complex, which assists placement of XPC–HR23B and TFIIH factors on DNA. Although NER has been studied intensively, contradictory data are still not explained unambiguously; however, these contradictions disappear in the framework of the random order assembly model [15, 16]. According to this model, a lesion is initially detected by any of these proteins (XPA, RPA, or XPC–HR23B) providing assembly of a four-component complex on the damaged DNA due to cooperative protein–protein interactions; this complex includes TFIIH factor, which kinetically checks specificity of the complex.

Besides the fact that the NER mechanism is ambiguous, details of the interaction of certain participants in the process with damaged DNA are also unclear. Earlier we showed that it is possible to use oligonucleotides bearing bulky photoreactive nucleotide analogs as substrates recognized by the NER system. It was demonstrated that bulky photoreactive nucleotide analogs inserted in DNA substrates are recognized and processed by UvrABC proteins of the bacterial NER system and also by the human NER system [17, 18]. Use of lesion-imitating photoreactive groups allows covalent fixation of the polypeptide in direct contact with photoreactive DNA damage. However, in this case it is unclear what protein factors of the NER system are in contact with the undamaged DNA strand in the course of damage recognition. To solve this problem, we constructed DNA duplexes bearing 5I-dUMP in the undamaged strand and Flu-dUMP as a lesion in the other strand (Fig. 1). Choice of photoreactive nucleotide analog is motivated by the hypothesis of its minimal effect on the structure of DNA double helix. In this work, we studied the interaction of NER protein factors—RPA, XPA, and XPC–HR23B—with model DNA structures imitating NER substrates.

MATERIALS AND METHODS

The following materials and reagents were used: [γ-^{32}P]ATP (3000 Ci/mmol) produced in the Laboratory of Radiochemistry of the Institute of Chemical Biology and Fundamental Medicine (Siberian Branch of the Russian Academy of Sciences); phage T4 polynucleotide kinase from Biosan (Russia); stained molecular mass markers from BioRad (USA); reagents for electrophoresis and buffer components from Sigma (USA) or of Russian production (extra pure grade).

Oligonucleotides bearing 5I-dUMP or fluorescein dUMP derivative were synthesized by the solid phase method using corresponding commercially available amidophosphites from Glen Research (USA). Structures of oligonucleotides and nucleotide analogs are presented in Fig. 1.

Protein preparations. Recombinant hRPA was isolated from *E. coli* according to [19]. Recombinant hXPA bearing N-terminal polyhistidine fragment was expressed in *E. coli* BL21(DE3)LysS strain, using pET15b-XPA recombinant plasmid. Cells were disintegrated ultrasonically, and after centrifugation the cleared lysate was applied on a column with Ni-chelate agarose equilibrated with buffer A (50 mM potassium phosphate, pH 7.8, 0.1 M NaCl, 0.001% NP-40, and 10% glycerol) with 5 mM imidazole. The target protein was eluted with buffer A containing 100 mM imidazole, eluate was fractionated, and fractions containing the main content of the protein were pooled. After addition of EDTA (to 1 mM) and 2-mercaptoethanol (to 7 mM), the pooled fraction was applied on a column with Sephacryl S-200 equilibrated with buffer B (25 mM Tris-HCl, pH 7.8, 0.1 M NaCl, 1 mM EDTA, 7 mM 2-mercaptoethanol, and 10% glycerol), which was also used for elution. After gel filtration, XPA-containing fractions were pooled and applied on a column with heparin-Sepharose equilibrated with buffer B. The protein was eluted with a gradient (0.1-1.0 M) of NaCl in buffer B. The main content of protein was eluted in the NaCl concentration range 0.55-0.75 M.

a

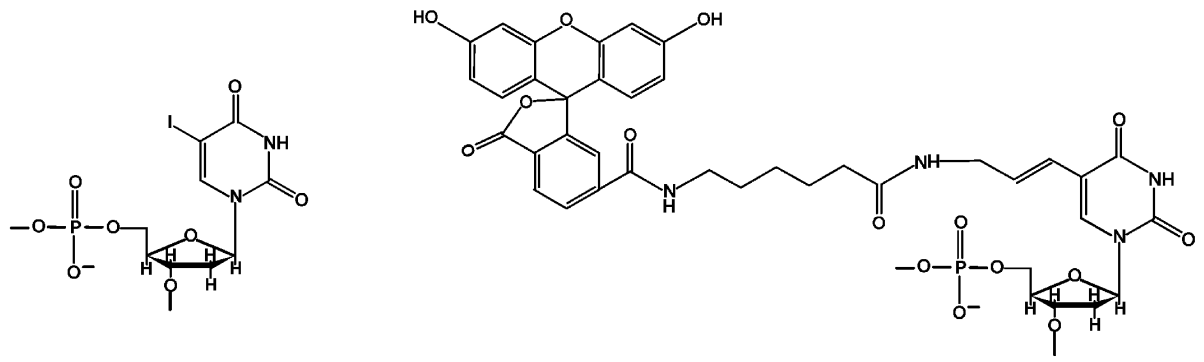

5-IdUMP

5-iodo-2′-deoxyuridine 5′-monophosphate

Flu-dUMP

5-{3-[6-(carboxyamido-fluoresceinyl)amidocapro-moyl]allyl}-2′-deoxyuridine 5′-monophosphate

b

```
5'-p*-CTAT GGCG AGGC GATT AAGT TGGG CAAC GUCA GGGT CTTC CGAA CGAC-3′
   3′-GATA CCGC TCCG CTAA TTCA ACCC GTTG CAGT CCCA GAAG GCTT GCTG-5′
```

DNA 1

```
5'-p*-CTAT GGCG AGGC GATT AAGT TGGG C AAC GUCA GGGT CTTC CGAA CGAC-3′
   3′-GATA CCGC TCCG CTAA TTCA ACCC A FTG CAGT CCCA GAAG GCTT GCTG-5′
```

DNA 2

```
5'-p*-CTAT GGCG AGGC GATT AAGT TGGG CAAC GUCA GGGT CTTC CGAA CGAC-3′
   3′-GATA CCGC TCCG CTAA TTCA ACCC GFTG CAGT CCCA GAAG GCTT GCTG-5′
```

DNA 3

```
5′-p*-CTAT GGCG AGGC GAUT AAGT TGGG C AAC GTCA GGGT CTTC CGAA CGAC-3′
   3′-GATA CCGC TCCG CTAA TTCA ACCC A FTG CAGT CCCA GAAG GCTT GCTG-5′
```

DNA 4

```
5′-p*-CTAT GGCG AGGC GATT AAGU TGGG C AAC GTCA GGGT CTTC CGAA CGAC-3′
   3′-GATA CCGC TCCG CTAA TTCA ACCC A FTG CAGT CCCA GAAG GCTT GCTG-5′
```

DNA 5

```
5′-p*-CTAT GGCG AGGC GATT AAGT TGGG U AAC GTCA GGGT CTTC CGAA CGAC-3′
   3′-GATA CCGC TCCG CTAA TTCA ACCC G FTG CAGT CCCA GAAG GCTT GCTG-5′
```

DNA 6

```
5′-p*-CTAT GGCG AGGC GATT AAGT TGGG C AAC GTCA GGGU CTTC CGAA CGAC-3′
   3′-GATA CCGC TCCG CTAA TTCA ACCC A FTG CAGT CCCA GAAG GCTT GCTG-5′
```

DNA 7

U=5-IdUMP F=Flu-dUMP

Fig. 1. Structures of nucleotide analogs (a) and sequences of DNA duplexes used in this work (b).

The pooled fraction was dialyzed against two portions of buffer B in which glycerol was added to 20%. The resulting preparation was aliquoted and stored at −40°C. The yield of protein was 0.05-0.1 mg for 1 g of biomass.

Recombinant hXPC–HR23B bearing polyhistidine sequence at the C-end of hXPC and at the N-end of HR23B was purified as described in [18]. The mutant RPA without domains responsible for protein–protein interactions was kindly provided by Alexey Bochkarev from the University of Toronto (Canada), and *E. coli* SSB protein was kindly provided by Stephen Kowalczykowski from the University of California (USA).

Preparation of 5′-^{32}P-labeled DNA duplexes. Radioactive label was inserted into the 5′-end of 5I-dUMP-containing oligonucleotides using phage T4 polynucleotide kinase as described in [20]. Labeled oligonucleotides were purified by electrophoresis under denaturing conditions with subsequent elution [21]. To obtain DNA duplexes, 5′-^{32}P-labeled oligonucleotides were annealed with complementary oligonucleotides in the ratio 1 : 1.2, incubated for 5 min at 95°C, then slowly cooled to 70°C, kept for 15 min at this temperature, and slowly cooled to room temperature. The hybridization degree was monitored by electrophoresis in 7% polyacrylamide gel (acrylamide/bis-acrylamide = 40 : 1). TBE buffer (50 mM Tris-HCl, 50 mM H_3BO_3, 1 mM EDTA, pH 8.3) was used as the electrode buffer.

Protein binding to DNA was analyzed by gel retardation. The reaction mixture (10 μl) contained 50 mM Tris-HCl, pH 7.5, 100 mM KCl, 2 mM $MgCl_2$ (if the reaction was performed in the presence of Mg^{2+}), 1 mM dithiothreitol (DTT), 0.6 mg/ml BSA, 1 nmol 5′-^{32}P-labeled DNA, and RPA, XPA, or XPC–HR23B at various concentrations. Protein complexes with DNA were formed for 30 min at 37°C. Then loading buffer (1 : 5 v/v) containing 20% glycerol and 0.015% Bromophenol Blue was added to the sample. Protein–nucleic acid complexes were electrophoresed under nondenaturing conditions. To separate the products of complex formation of RPA, XPA, or their mixtures, 7% polyacrylamide gel (acrylamide/bis-acrylamide = 40 : 1) was used, whereas for XPC–HR23B or protein mixtures containing it, 5% polyacrylamide gel (acrylamide/bis-acrylamide = 60 : 1) was used. TBE was used as the electrode buffer. Electrophoresis was performed with voltage decrease 17 V/cm and at 4°C. Positions of radioactively labeled oligonucleotide and protein–nucleic acid complexes were determined autoradiographically using a Molecular Imager FX Pro+ from BioRad.

Photoaffinity labeling of proteins by photoreactive DNA structures was performed in reaction mixture (10 μl) containing 50 mM Tris-HCl, pH 7.5, 100 mM KCl, 2 mM $MgCl_2$ (if the reaction was performed in the presence of Mg^{2+}), 1 mM DTT, 0.6 mg/ml BSA, 10 nM 5′-^{32}P-labeled photoreactive DNA duplex, and corresponding protein or protein mixture at the studied concentrations. Mixtures were incubated for 30 min at 37°C and then UV-irradiated in an ice bath using a Bio-Link BLX-312 cross-linker from Vilber Lourmant (France) at wavelength 312 nm, light intensity 5 mJ/cm^2·sec, and irradiation time 1 h. The reaction was terminated by addition of stop buffer (1 : 5 v/v) (5% SDS, 5% 2-mercaptoethanol, 0.3 M Tris-HCl, pH 7.8, 50% glycerol, and 0.005% Bromophenol Blue). Modification products were separated by electrophoresis according to Laemmli [22] with subsequent autoradiography using the Molecular Imager FX Pro+ (Bio-Rad).

RESULTS AND DISCUSSION

To study the interaction of NER factors with DNA, we used 48-mer DNA duplexes bearing a bulky damage in one strand and a photoactive 5I-dUMP analog in the opposite strand. dUMP analog bearing base-attached fluorescein residue (Flu-dUMP) was used for damage imitation. Being inserted into DNA, this analog is recognized as a damage repaired by the NER system [23]. The iodine atom in 5I-dUMP chromophore has Van der Waals radius very close to that of the methyl group of thymidine. Due to this similarity with the natural nucleotide, this analog causes minimal changes in DNA helix and therefore in formation of protein–nucleic acid complexes. It is suggested that a photoreactive group bound with a linker of "zero" length should react only with amino acid residues in close contact with DNA [24]. The DNA strand bearing a photoactive analog contained 5′-^{32}P-label. Structures of dUMP analogs and sequences of DNA duplexes are presented in Fig. 1.

Complex formation of NER factors with various DNA structures. The affinity of NER factors to DNA structures used was evaluated by gel retardation. Experiments on RPA binding to various DNA structures (Fig. 2) showed that RPA affinity to undamaged DNA 1 is minimal both in the absence (Fig. 2a, lanes *1-7*) and in the presence (Fig. 2b, lanes *1-6*) of Mg^{2+}. However, between damaged DNA 2 and DNA 3 in the presence of 2 mM Mg^{2+}, RPA demonstrates the maximal affinity to DNA 2 bearing a non-complementary base pair along with a damage (Fig. 2b, lanes *7-11*). In the absence of Mg^{2+}, RPA binds to all DNA structures more efficiently, but the difference in protein affinity to DNA 2 and DNA 3 is minimized, as shown in the plots of complex formation versus protein concentration (Fig. 2, a and b, right parts). The character of RPA complex formation with damaged DNA also depends on the presence of Mg^{2+} in the reaction mixture: in the absence of Mg^{2+} several types of RPA–DNA complexes with various electrophoretic mobility are observed, whereas in the presence of Mg^{2+} DNA 2 and DNA 3 mainly form complexes with lower electrophoretic mobility (Fig. 2a, lanes *10*, *11* and *16*, *17* versus Fig. 2b, lanes *8*, *9* and *14*, *15*). Complexes of this type are formed when

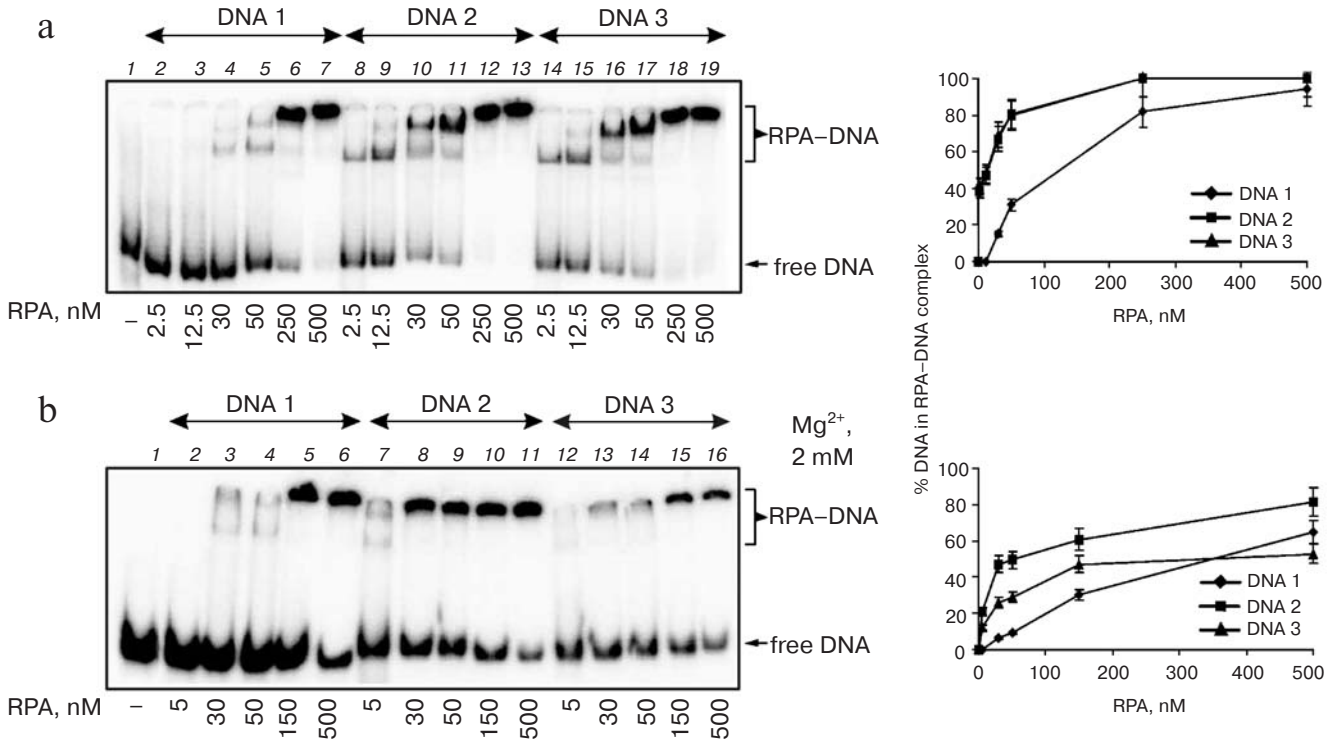

Fig. 2. RPA binding to various DNA structures in the absence (a) and in the presence (b) of 2 mM Mg^{2+}. The reaction mixtures contained 50 mM Tris-HCl, pH 7.5, 100 mM KCl, 2 mM $MgCl_2$ (if the reaction was performed in the presence of Mg^{2+}), 1 mM DTT, 0.6 mg/ml BSA, 1 nM of 5′-^{32}P-labeled DNA, and RPA at various concentrations. Lanes: *1-7*) undamaged DNA duplex (DNA 1); *8-13*) DNA duplex bearing a non-complementary base pair along with a damage (DNA 2); *14-19*) damaged DNA duplex (DNA 3).

DNA binds to several protein molecules, and the fact that they are mainly formed in the presence of free DNA in solution indicates that cooperativity is enhanced on RPA binding to the damaged DNA in the presence of Mg^{2+}. The character of RPA binding to undamaged DNA is practically independent on the presence of Mg^{2+} (Fig. 2a, lanes *4*, *5* versus Fig. 2b, lanes *3*, *4*). The effect of Mg^{2+} on the ability of RPA for selective binding to UV-irradiated DNA was first shown in [25]; the data suggest that the role of RPA is primary recognition of damage. The ability of RPA to recognize DNA duplexes with various damages is as shown in [25-33]. Data on RPA binding to single-stranded damaged DNA obtained by various methods differ significantly, demonstrating preferential binding to damaged compared to undamaged DNA [26, 35], as well as the opposite effect [27, 29, 34, 36].

For a long time XPA was the main candidate for the role of damage-recognizing factor. This protein was the first discovered NER participant, which demonstrated preferential binding to damaged DNA [29, 37]. However, after the discovery of other participants of the NER system it became obvious that XPA binding specificity to the damaged DNA is negligible, and most probably this protein does not directly participate in damage recognition, but together with RPA coordinates assembly of pre-incision complex via protein–protein interactions with all of its participants [14]. Data on XPA binding to DNA duplexes used in this work are presented in Fig. 3a. As can be seen, XPA demonstrates some preference in binding to DNA duplexes bearing damage repaired by NER system (lanes *7-11* and *12-16*) compared with undamaged DNA (lanes *2-6*). The presence of Mg^{2+} in the reaction mixture results in significant inhibition of XPA binding to any DNA structures (data not presented), which is in complete accord with [29].

A heterodimer XPC–HR23B is fully accepted as the main factor of primary recognition of damage [13]. According to [38], XPC–HR23B has high affinity to DNA double helix sites, whose structure is destabilized by bulky damages. To our surprise, in binding experiments (Fig. 3b) we observed only a negligible preference in XPC–HR23B binding to damage-bearing DNA structures (DNA 2, lanes *7-11*) or the same substituent near the non-complementary base pair (DNA 3, lanes *12-16*) compared with undamaged DNA (lanes *2-6*). In the presence of Mg^{2+}, the level of complex formation significantly decreases. However, the picture in principle remained the same (data not presented). So, the data indicate that any one of the NER factors taken separately does not demonstrate noticeable preference in binding to damaged

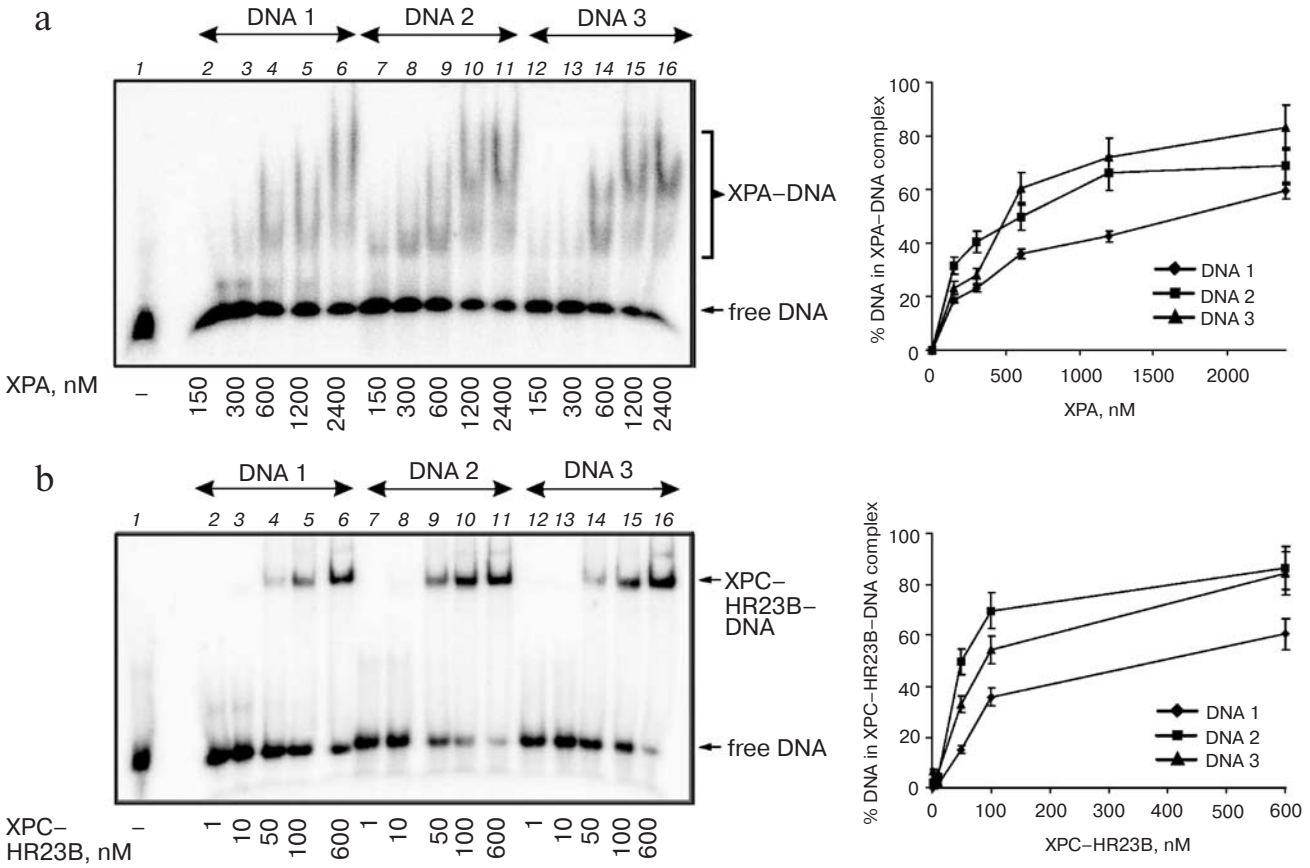

Fig. 3. XPA (a) and XPC–HR23B (b) binding to various DNA structures. The reaction mixtures contained 50 mM Tris-HCl, pH 7.5, 100 mM KCl, 1 mM DTT, 0.6 mg/ml BSA, 1 nM 5′-^{32}P-labeled DNA, and proteins at various concentrations.

DNA necessary for discrimination of DNA damages on the background of the main part of undamaged DNA. Therefore, the discrimination mechanism is more complicated and requires participation of several proteins simultaneously and/or other factors governing discrimination.

Interaction of various NER factors on DNA binding. Several NER factors participate in recognition of DNA damages, and this process is regulated by numerous protein–nucleic acid and protein–protein interactions. Each of these specific interactions is necessary for functioning of the whole system. Study of the interaction between NER factors is necessary for understanding their role in DNA damage recognition. To evaluate the effect of RPA on XPC–HR23B binding to the studied DNA duplexes, we titrated DNA with XPC–HR23B heterodimer in the absence and in the presence of RPA. Figure 4a presents data on DNA 2 titration with XPC–HR23B in the absence of RPA (lanes *7-9*) and in the presence of 1 nM (lanes *10-13*) and 5 nM (lanes *2-6*) RPA. Under the experimental conditions RPA forms two types of RPA–DNA complexes with different electrophoretic mobility. Due to the lower electrophoretic mobility of XPC–HR23B–DNA complex, it is possible to separate the products of RPA and XPC–HR23B complex formation with DNA. In the presence of 5 nM RPA, a band corresponding to XPC–HR23B–DNA complex appears at XPC–HR23B concentration 5 nM (lane *5*), whereas in the presence of 1 nM RPA (lane *12*) or in its absence (lane *8*) this complex is not formed at the same XPC–HR23B concentration. Figure 4b presents data on titration of all DNA duplexes used with XPC–HR23B heterodimer in the presence of 5 nM RPA (DNA 1, lanes *4-6*; DNA 2, lanes *10-12*; DNA 3, lanes *16-18*). At 25 nM XPC–HR23B in the reaction mixture, signal intensity of the products of XPC–HR23B complex formation with DNA is significantly higher in the presence of RPA (lanes *6*, *12*, *18*) than in its absence (lanes *7*, *13*, *19*). The data suggest that RPA stimulates XPC–HR23B binding to various DNA structures. At increased XPC–HR23B concentration the intensity of bands corresponding to RPA–DNA complex decreases; this possibly arises from formation of RPA–XPC–HR23B–DNA triple complex. However, the absence of additional bands in gel that might be related with such complex suggests that RPA stimulates XPC–HR23B binding to DNA due to protein–protein interactions without formation of a stable triple complex. The interaction between RPA and XPC

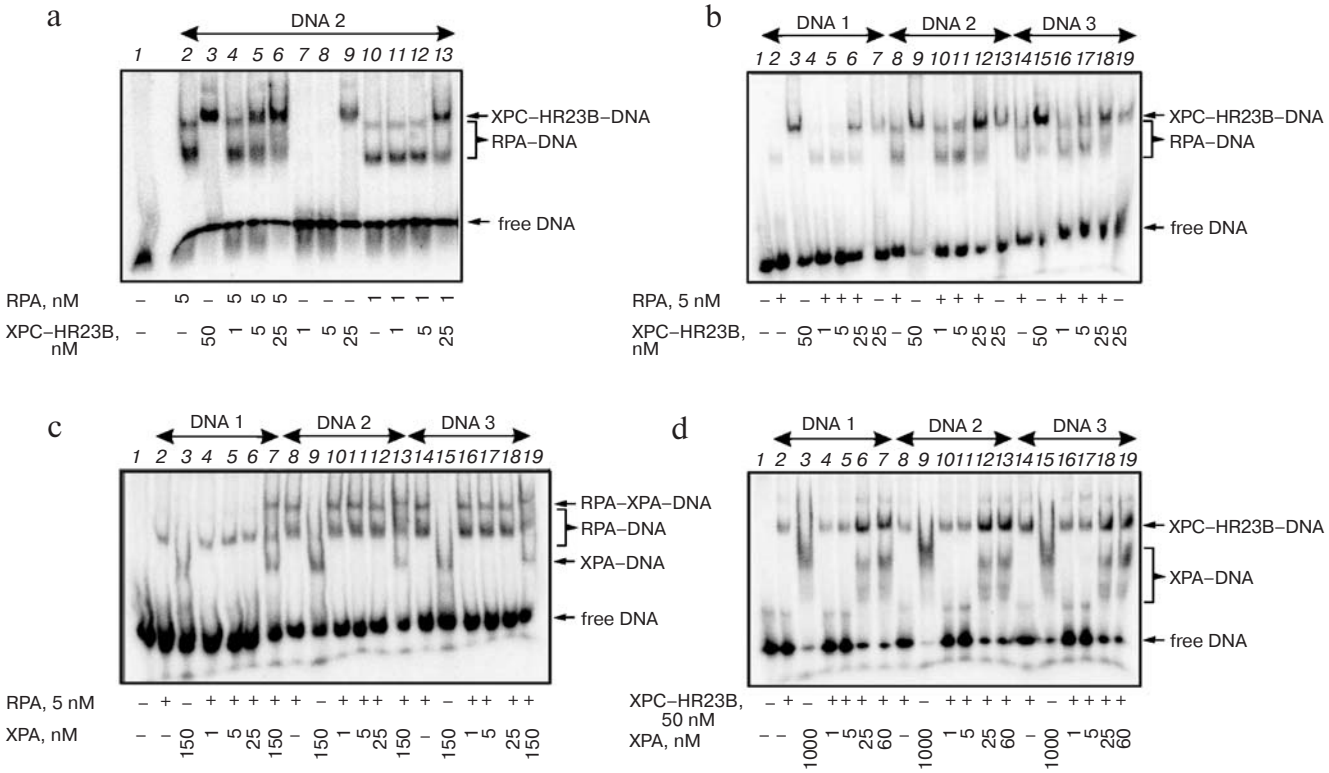

Fig. 4. Interaction of NER protein factors with DNA. The reaction mixtures contained 50 mM Tris-HCl, pH 7.5, 100 mM KCl, 1 mM DTT, 0.6 mg/ml BSA, 1 nM 5′-^{32}P-labeled DNA, and protein factors at analyzed concentrations: a) 1 or 5 nM RPA and XPC–HR23B at various concentrations; b) 5 nM RPA and XPC–HR23B at various concentrations; c) 5 nM RPA and XPA at various concentrations; d) 50 nM XPC–HR23B and XPA at various concentrations.

subunit expressed as chimeric polypeptide with maltose-binding protein (MBP–XPC) on binding to UV-damaged DNA was studied by gel retardation [14]; however, neither stimulation effect nor formation of DNA–protein triple complex were detected. However, the interaction between RPA and MBP–XPC on binding to DNA was detected by footprinting. That is why the mechanism of interaction of these proteins remains unclear.

The formation of XPA_2–RPA complex was discovered earlier [14, 36, 39], and it was shown that this complex has higher affinity to damaged DNA than XPA and RPA taken separately [40, 41]. In our experiments on XPA titration in the presence of RPA at constant concentration (Fig. 4c), a band corresponding to XPA–RPA–DNA complex appeared at RPA/XPA concentration ratio 1 : 30 (lanes *7*, *13*, *19*). At XPA concentration lower than 150 nM only the bands corresponding to RPA–DNA complex were observed (DNA 1, lanes *4-6*; DNA 2, lanes *10-12*; DNA 3, lanes *16-18*). The presence of Mg^{2+} in the reaction mixture results in a dramatic decrease in the amount of XPA–DNA complex, which causes disappearance of a band corresponding to the triple complex (data not presented here).

Data on XPA binding to DNA in the presence of XPC–HR23B at constant concentration are presented in Fig. 4d. On increase of XPA concentration, simultaneous increase in intensity of the bands corresponding to the products of XPC–HR23B complex formation was observed (DNA 1, lanes *4-7*; DNA 2, lanes *10-13*; DNA 3, lanes *16-19*). The data indicate that XPA stimulates formation of XPC–HR23B–DNA complex. Increased XPA concentration in the protein mixture changes the number of products of complex formation as well as the ratio of their intensities. At XPA concentrations 1 and 5 nM (DNA 1, lanes *4*, *5*; DNA 2, lanes *10*, *11*; DNA 3, lanes *16*, *17*) only the bands corresponding to XPC–HR23B–DNA complex were observed; this arises from the higher affinity of XPC–HR23B to DNA. However, already at 25 nM XPA distinct bands corresponding to XPA–DNA complex (lanes *6*, *12*, *18*) appear simultaneously with drastic increase in intensity of the band of the XPC–HR23B–DNA complex, whereas in the absence of XPC–HR23B such complexes were observed only at significantly higher XPA concentrations (Fig. 3a). So these NER factors mutually stimulate their binding to DNA. For all DNA duplexes used, this effect manifests itself to an equal extent. It is possible that XPC–HR23B–XPA–DNA complex is formed; however, we failed to detect such complex in our experiments. The presence of Mg^{2+} in the reaction mixture does not change

the stimulation effect (data not presented). Interactions between XPC–HR23B and XPA in the course of their binding to UV-damaged DNA duplex was found earlier by footprinting [14].

Study of interaction of NER factors by photoaffinity modification. Our data on formation of XPA–RPA–DNA triple complexes obtained in experiments on XPA or RPA binding to DNA by gel retardation are in complete agreement with the literature data. The fact that XPA–RPA complex can be isolated from HeLa cell extract [42] indicates that XPA and RPA interact in the absence of DNA and that this complex might be functionally important. However, in spite of intense study and many data obtained by various methods, the role of the separate protein components of XPA–RPA complex in binding to damaged DNA is still unclear. Photoaffinity modification was used for analysis of the location of subunits of this complex on DNA. This method can be used to detect weak protein–nucleic acid interactions, which are crucial for many biological processes.

Modification of XPA revealed an unexpected phenomenon: DNA structures we used did not modify this protein even in its excess (XPA/DNA ratio up to 200 : 1), furthermore, on addition of RPA, the set and intensities of the products of protein mixture modification completely corresponded with the products of RPA modification, in particular its major subunit RPA70 (data not presented). This fact might be due either to the absence of the appropriate amino acid acceptors at the points of XPA–DNA contact or the absence of protein contacts with undamaged DNA strand. Interactions of XPA and RPA with DNA duplex bearing *cis*-dichlorodiammineplatinum as damage and 5I-dUMP photoactive analog in one strand were studied in [35]; it was shown that XPA–RPA–DNA triple complex exists and only the RPA70 subunit is subject to modification in this complex. It was suggested in [43] that on binding to the damaged DNA duplex XPA is positioned on the damaged strand at the 5′-side of the damage. Our data and the literature indicate that on binding of XPA–RPA complex to the damaged DNA duplex, only RPA contacts with the damage-bearing DNA site as well as with the area of the undamaged strand complementary to it. XPA is known to have high affinity to bends of DNA helix [44]; this fact suggests its binding to DNA after placement of XPC–HR23B, which produces a bend of the DNA duplex in the damaged area.

Data on electrophoretic separation of the products of modification of RPA and XPC–HR23B mixture by photoreactive DNA duplexes are presented in Fig. 5. Proteins were modified at increased XPC–HR23B concentration in the presence of 50 nM RPA and one of the DNA structures. The products of labeling corresponding to XPC–HR23B–DNA complex are absent from lanes *3*, *9*, *15* containing XPC–HR23B and DNA. At concentration ratio XPC–HR23B/RPA = 8 : 1, bands corresponding to XPC–HR23B modification products appear (lanes *7*, *13*, *19*). The XPC–HR23B concentration in these lanes are the same as in lanes containing only XPC–HR23B and DNA. The data indicate that RPA stimulates an interaction between XPC–HR23B and DNA and support data obtained by gel retardation. The intensity of RPA modification decreases simultaneously with appearance of the products of XPC–HR23B modification. The stimulating effect of RPA manifests itself most clearly in the case of DNA bearing non-complementary nucleotides in the vicinity of the damage (lanes *8-13*). It should be noted that intensity and character of RPA labeling also depend on DNA structure. Thus, on interaction with DNA 1 not only lower yield of DNA–protein conjugates is observed as compared with DNA 2 and DNA 3, but the set of products of RPA modification also differs (lane *2* versus lanes *8* and *14*). The number of labeling products of RPA subunits is larger in the case of damaged DNA; this may be related with conformational rearrangements of protein in complex with such DNA, which increases the number of potential target amino acids for photoinduced DNA crosslinking.

To clarify the suggestion of a role of protein–protein contacts in RPA-induced stimulation of XPC–HR23B interaction with DNA, we performed experiments on photoaffinity modification of XPC–HR23B in the presence of an RPA mutant form depleted of all domains responsible for protein–protein interactions (data not presented). The absence of any effect of this mutant RPA on XPC–HR23B modification indicates that the mutant form of RPA is unable to stimulate the interaction of XPC–HR23B with DNA. The data indicate that the observed stimulating effect is based on protein–protein interactions between RPA and XPC–HR23B. The specificity of interaction between RPA and XPC–HR23B was demonstrated in experiments on photoaffinity modification of XPC–HR23B in the presence of a prokaryotic RPA analog—SSB protein of *E. coli*. Replacement of

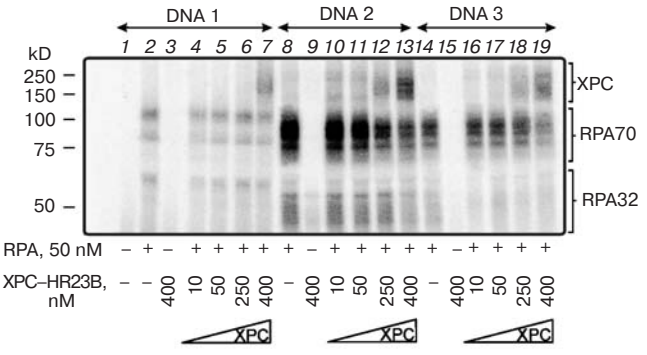

Fig. 5. Photoaffinity modification of XPC–HR23B in the presence of RPA. The reaction mixtures contained 50 mM Tris-HCl, pH 7.5, 100 mM KCl, 1 mM DTT, 0.6 mg/ml BSA, 50 nM RPA, XPC–HR23B at various concentrations, and 10 nM 5′-^{32}P-labeled photoreactive DNA (DNA 1, 2, or 3).

RPA by SSB in the reaction mixture resulted in complete disappearance of the stimulating effect of XPC–HR23B labeling.

It is known that the interaction of RPA with single-stranded DNA is polar [32, 45]; it was also shown that RPA mainly binds to damaged DNA at the 5′-side of the damage [35]. Since it was found that RPA preferentially binds to the undamaged strand of DNA duplex [46], it was of interest to study protein localization on undamaged DNA strand and to evaluate its effect on the interaction of XPC–HR23B factor with various DNA sites. Data on modification of proteins by DNA duplexes different in position of a 5I-dUMP residue in the undamaged strand (DNA 2, DNA 4-DNA 7) are presented in Fig. 6. As can be seen, the level and character of RPA labeling depend on the position of a photoreactive analog in relation to the damaged site. The highest modification is observed for DNA 4 and 7 (lanes *2*, *14*); this may be rationalized by the position of the photoactive analog in the DNA area, which contacts the high-affinity DNA-binding domains A and B of RPA. In DNA 4, a photoreactive analog is located at the 5′-side of the damage, whereas in DNA 7 it is at the 3′-side of the damage. The equal level of RPA modification by these structures can be rationalized by binding of two protein molecules to DNA duplex; one of these protein molecules interacts mainly with the 5′-terminal area of the undamaged DNA strand (DNA 4), and the other with the 3′-terminal area (DNA 7). Of several products of modification of RPA70 subunit by DNA 4 and 7, the highest level of labeling corresponds with the products with higher electrophoretic mobility. As for DNA–protein adducts of RPA70 with DNA 2 (lane *11*), the higher level of labeling corresponds with the products with lower electrophoretic mobility. The yields of products of RPA affinity modification by DNA duplexes 5 and 6 are nearly equal (lanes *5*, *8*), although the character of labeling differs. So, dependent on the position of the photoreactive group in the undamaged strand, the character

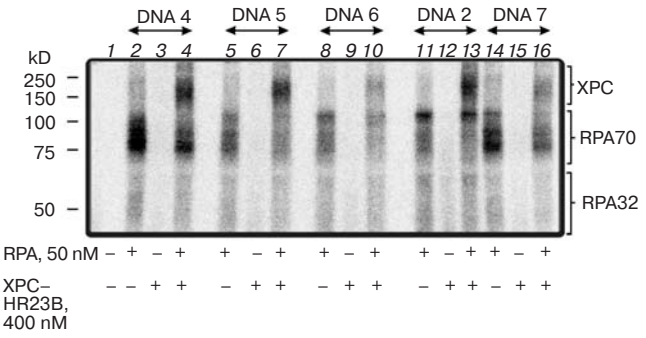

Fig. 6. Photoaffinity modification of XPC–HR23B in the presence of RPA by DNA structures bearing 5I-dUMP at various positions in relation to the damaged site. The reaction mixtures contained 50 mM Tris-HCl, pH 7.5, 100 mM KCl, 1 mM DTT, 0.6 mg/ml BSA, 50 nM RPA, 400 nM XPC–HR23B, and 10 nM 5′-^{32}P-labeled photoreactive DNA.

and intensity of RPA labeling differ; this might be due to the modification of different areas of the protein or even different protein molecules. As shown above (Fig. 2), RPA binding to damaged DNA is highly cooperative, and this results in placement of several protein molecules on one DNA molecule. In such complexes, RPA has globular conformation [47] and interacts with DNA mainly via DNA-binding domains A and B of the RPA70 subunit [48, 49]. Placement of RPA in the extended conformation, when other DNA-binding domains are also involved in interaction with DNA, seems to be realized already in the opened complex after DNA unwinding around damage by DNA helicases XPB and XPD of multisubunit factor TFIIH ([3] and references cited therein). Such placement provides polar RPA location on DNA necessary for a proper orientation of excision nucleases XPG and ERCC1-XPF catalyzing incision of the damaged DNA site [3, 32].

Study of the effect of RPA on XPC–HR23B labeling (XPC–HR23B/RPA = 8 : 1) by DNA structures bearing damage, non-complementary nucleotides, and photoreactive analog at various positions of the undamaged strand showed that modification profile (dependence of modification intensity on position of photoreactive analog) of these proteins is different. The stimulating effect of RPA on XPC–HR23B modification manifests itself most clearly in the case of DNA 2 and 4 (lanes *4*, *13*). Use of DNA structure bearing a photoreactive analog at the position nearest to the damage (DNA 6) results in the lowest level of cross-linking for RPA (lane *8*) as well as for XPC–HR23B in the protein mixture (lane *10*). This might be caused by the fact that in this structure, the 5I-dU residue is located opposite to dG but not in the canonical pair with dA; this might influence the spatial orientation of the photoreactive group and respectively, the efficiency of protein modification. An interesting result was obtained for DNA 7—the level of RPA modification by this structure is one of the highest (lane *14*), whereas use of this structure for modification of a protein mixture results in drastic decrease in level of RPA labeling and low cross-linking to XPC–HR23B (lane *16*). It is possible that after placement on DNA stimulated by RPA, XPC–HR23B displaces RPA from the DNA, and displacement from various DNA sites may occur unevenly, XPC–HR23B modification is dependent on the position of the photoreactive group. Based on biochemical experiments, it was recently suggested that XPC–HR23B interacts not with damage but with a site of the undamaged strand opposite to the damage [50, 51]. This hypothesis was supported by X-ray analysis of a complex of yeast ortholog XPC, Rad4, with a fragment of damaged DNA [52]. It should be noted that on modification of RPA and XPC–HR23B mixture by all DNA structures used, the level of RPA labeling significantly decreases simultaneously with appearance of the products of XPC–HR23B modification (lanes *2*, *5*, *8*, *11*, *14* containing only RPA versus lanes *4*, *7*, *10*, *13*, *16* con-

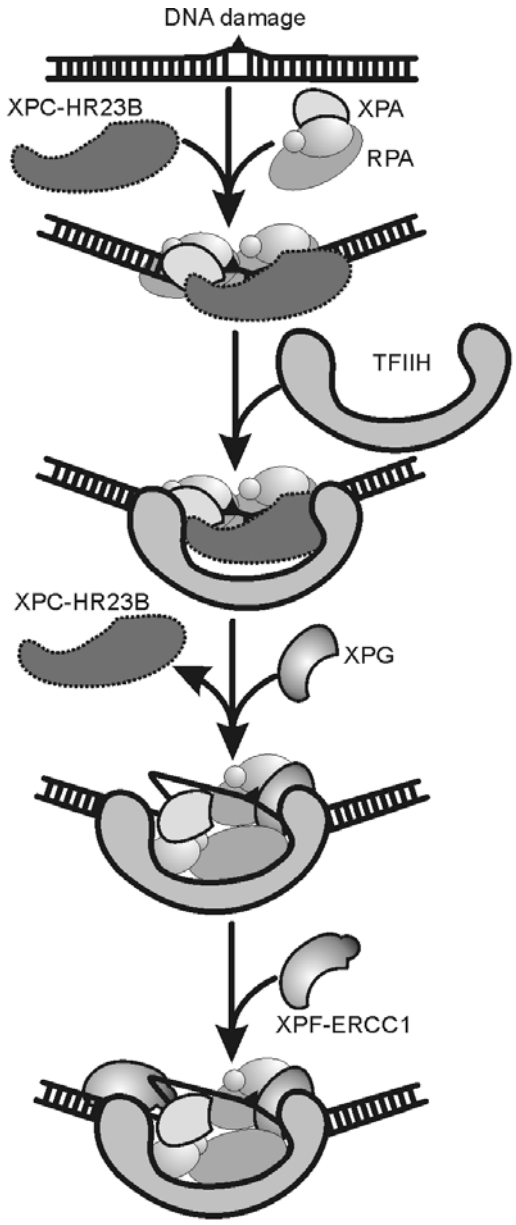

Fig. 7. Hypothetical model of assembly of pre-incision complex on damaged DNA during nucleotide excision repair.

taining a mixture of proteins). Thus, RPA and XPC–HR23B compete for the undamaged DNA strand. Therefore, our data on localization of XPC–HR23B factor on damaged DNA obtained by affinity modification are in accordance with the X-ray data.

So, our data demonstrate a negligible preference in binding of all studied NER factors taken separately, including that of XPC–HR23B to damaged DNA compared with native DNA duplex. At the present time XPC–HR23B is considered to be the most probable factor providing primary recognition of DNA damages. We have found that RPA and XPA stimulate the interaction of XPC–HR23B with DNA. The effect of RPA and XPA on XPC–HR23B binding to DNA is practically independent of the type of DNA duplex, whereas the effect on photoinduced cross-linking manifests itself to the maximal degree in case of DNA bearing a bulky substituent. Earlier we obtained analogous results on the effect of these proteins on the efficiency of XPC–HR23B modification, studying the interaction of NER factors with 60-mer DNA duplexes bearing bulky photoreactive nucleotide derivatives as damage [18]. Based on all of the data, conclude that despite the common opinion that XPC–HR23B is a factor providing primary recognition of damage in DNA, participation of RPA and XPA in this process cannot be excluded. Our data most likely indicate cooperative binding of proteins participating in formation of pre-incision complex to the damaged DNA [15, 16]. A hypothetical model of formation of this complex accounting for possible cooperative interactions of RPA, XPA, and XPC–HR23B factors is presented in Fig. 7.

This work was financially supported by the Russian Foundation for Basic Research (grant Nos. 06-04-48526, RFBR-JSPS 08-04-91202, RFBR-DFG 08-04-91973), grant HFSP RGP 0007/2004-C104, grant INTAS-SBRAS 06-1000013-9210, and by grants from program "Leading Scientific Schools" (652.2008) and RAS program on Molecular and Cell Biology.

REFERENCES

1. Sancar, A. (1996) *Ann. Rev. Biochem.*, **65**, 43-81.
2. Wood, R. D. (1997) *J. Biol. Chem.*, **272**, 23465-23468.
3. De Laat, W. L., Jaspers, N. G., and Hoeijmakers, J. H. (1999) *Genes Dev.*, **13**, 768-785.
4. Friedberg, E. C., Walker, G. C., and Siede, W. (1995) *95th Ann. Meet. of the Amer. Soc. Microbiol.*, ASM Press, Washington DC, USA.
5. Kraemer, K. H., Lee, M. M., and Scott, J. (1984) *Carcinogenesis*, **5**, 511-514.
6. States, J. C., McDuffie, E. R., Myrand, S. P., McDowell, M., and Cleaver, J. E. (1998) *Hum. Mutat.*, **12**, 103-113.
7. Cleaver, J. E., Thompson, L. H. A., Richardson, A. S., and States, J. C. (1999) *Hum. Mutat.*, **14**, 9-22.
8. Bohr, V. A., Smith, C. A., Okumoto, D. S., and Hanawalt, P. C. (1985) *Cell*, **40**, 359-369.
9. Gillet, L. C. J., and Scharer, O. D. (2006) *Chem. Rev.*, **106**, 253-276.
10. Mellon, I., Spivak, G., and Hanawalt, P. C. (1987) *Cell*, **51**, 241-249.
11. Mellon, I., and Hanawalt, P. C. (1989) *Nature*, **342**, 95-98.
12. Evans, E., Moggs, J. G., Hwang, J. R., Egly, J. M., and Wood, R. D. (1997) *EMBO J.*, **16**, 6559-6573.
13. Sugasawa, K., Ng, J. M., Masutani, C., Iwai, S., van der Spek, P. J., Eker, A. P., Hanaoka, F., Bootsma, D., and Hoeijmakers, J. H. (1998) *Mol. Cell*, **2**, 223-232.
14. Wakasugi, W., and Sancar, A. (1999) *J. Biol. Chem.*, **274**, 18759-18768.
15. Reardon, J. T., and Sancar, A. (2003) *Genes Dev.*, **17**, 2539-2551.

16. Kesseler, K. J., Kaufmann, W. K., Reardon, J. T., Elston, T. C., and Sancar, A. (2007) *J. Theor. Biol.*, **249**, 361-375.
17. Dellavecchia, M. J., Croteau, D. L., Skorvaga, M., Dezhurov, S. V., Lavrik, O. I., and van Houten, B. (2004) *J. Biol. Chem.*, **279**, 45245-45256.
18. Maltseva, E. A., Rechkunova, N. I., Gillet, L. C., Petruseva, I. O., Scharer, O. D., and Lavrik, O. I. (2007) *Biochim. Biophys. Acta*, **1770**, 781-789.
19. Henricksen, L. A., Umbricht, C. B., and Wold, M. S. (1994) *J. Biol. Chem.*, **269**, 11121-11132.
20. Sambrook, J., Fritsch, E. F., and Maniatis, T. (1989) *Molecular Cloning: A Laboratory Manual*, 2nd Edn., Cold Spring Harbor Laboratory Press, N. Y.
21. Yamshchikov, V. F. (1990) *Methods for Molecular Genetics and Gene Engineering* (Salganic, R. I., ed.) [in Russian], Nauka, Novosibirsk, pp. 145-154.
22. Laemmli, U. K. (1970) *Nature*, **227**, 680-685.
23. Nakano, T., Katafuchi, A., Shimizu, R., Terato, H., Suzuki, T., Tauchi, H., Makino, K., Skorvaga, M., van Houten, B., and Ide, H. (2005) *Nucleic Acids Res.*, **33**, 2181-2191.
24. Meisenheimer, K. M., and Koch, T. H. (1997) *Crit. Rev. Biochem. Mol. Biol.*, **32**, 101-140.
25. Burns, J. L., Guzder, S. N., Sung, P., Prakash, S., and Prakash, L. (1996) *J. Biol. Chem.*, **271**, 11607-11610.
26. Lao, Y., Gomes, X. V., Ren, Y., Taylor, J. S., and Wold, M. S. (2000) *Biochemistry*, **39**, 850-859.
27. Patrick, S. M., and Turchi, J. J. (1999) *J. Biol. Chem.*, **274**, 14972-14978.
28. He, Z., Henricksen, L. A., and Wold, M. S. (1995) *Nature*, **374**, 566-569.
29. Hey, T., Lipps, G., and Krauss, G. (2001) *Biochemistry*, **40**, 2901-2910.
30. Clugston, C. K., McLaughlin, K., Kenny, M. K., and Brown, R. (1992) *Cancer Res.*, **52**, 6375-6379.
31. Lao, Y., Lee, C. G., and Wold, M. S. (1999) *Biochemistry*, **38**, 3974-3984.
32. De Laat, W. L., Appeldoorn, E., Sugasawa, K., Weterings, E., Jaspers, N. G., and Hoeijmakers, J. H. (1998) *Genes Dev.*, **12**, 2598-2609.
33. Missura, M., Buterin, T., Hindges, R., Hubscher, U., Kasparkova, J., Brabec, V., and Naegeli, H. (2001) *EMBO J.*, **20**, 3554-3564.
34. Liu, Y., Yang, Z., Utzat, C. D., Liu, Y., Geacintov, N. E., Basu, A. K., and Zou, Y. (2005) *Biochemistry*, **385**, 519-526.
35. Schweizer, U., Hey, T., Lipps, G., and Krauss, G. (1999) *Nucleic Acids Res.*, **27**, 3183-3189.
36. Patrick, S. M., and Turchi, J. J. (2001) *J. Biol. Chem.*, **276**, 22630-22637.
37. Jones, C. J., and Wood, R. D. (1993) *Biochemistry*, **32**, 12096-12104.
38. Sugasawa, K., Okamoto, T., Shimizu, Y., Masutani, C., Iwai, S., and Hanaoka, F. (2001) *Genes Dev.*, **15**, 507-521.
39. Wang, M., Mahrenholz, A., and Lee, S. (2000) *Biochemistry*, **39**, 6433-6439.
40. Patrick, S. M., and Turchi, J. J. (2002) *J. Biol. Chem.*, **277**, 16096-16101.
41. Yang, Z., Liu, Y., Mao, L. Y., Zhang, J. T., and Zou, Y. (2002) *Biochemistry*, **41**, 13012-13020.
42. Matsuda, T., Saijo, M., Kuraoka, I., Kobayashi, T., Nakatsu, Y., et al. (1995) *J. Biol. Chem.*, **270**, 4152-4157.
43. Reardon, J. T., and Sancar, A. (2002) *Mol. Cell Biol.*, **22**, 5938-5945.
44. Camenish, U., Dip, R., Schumacher, S. B., Schuler, B., and Naegeli, H. (2006) *Nat. Struct. Mol. Biol.*, **13**, 278-284.
45. Kolpashchikov, D. M., Khodyreva, S. N., Khlimankov, D. Y., Wold, M. S., Favre, A., and Lavrik, O. I. (2001) *Nucleic Acids Res.*, **29**, 373-379.
46. Hermanson-Miller, I. L., and Turchi, J. J. (2002) *Biochemistry*, **41**, 2402-2408.
47. Blackwell, L. J., and Borowiec, J. A. (1994) *Mol. Cell Biol.*, **14**, 3993-4001.
48. Bochkarev, A., Pfuetzner, R. A., Edwards, A. M., and Frappier, L. (1997) *Nature*, **385**, 176-181.
49. Bochkareva, E., Belegu, V., Korolev, S., and Bochkarev, A. (2001) *EMBO J.*, **20**, 612-618.
50. Buterin, T., Meyer, C., Giese, B., and Naegeli, H. (2005) *Chem. Biol.*, **12**, 913-922.
51. Maillard, O., Solyom, S., and Naegeli, H. (2007) *PLoS Biol.*, **5**, e79.
52. Min, J.-H., and Pavletich, N. P. (2007) *Nature*, **449**, 570-575.